ASSESSMENT OF BONDED REPAIRS TO COMPOSITE PANELS REPRESENTATIVE OF WING STRUCTURE

Reewanshu Chadha[1], John G. Bakuckas, Jr. [1, a], John Z. Lin[2], Tim Labik[3], Michael Fleming[4] and Erick Espinar-Mick[5]

[a] Corresponding Author: john.bakuckas@faa.gov
[1] FAA William J. Hughes Technical Center, Atlantic City, NJ 08405, USA
[2] Boeing Research & Technology, Seattle, WA 98108, USA
[3] Drexel University, Philadelphia, PA 19104, USA
[4] Boeing Research & Technology, Ladson, SC 29456, USA
[5] Boeing Commercial Airplane, Everett, WA 98294, USA

Abstract: The Federal Aviation Administration (FAA) and The Boeing Company have been investigating the safety and structural integrity issues of bonded repair technology through testing and analysis using the Aircraft Beam Structural Test (ABST) fixture, an innovative structural test capability at the FAA William J. Hughes Technical Center. The program objectives are to characterize the fatigue and damage tolerance performance of bonded repairs subjected to simulated service load (SL) conditions and to evaluate the residual load capability of a typical composite wing panel of transport category aircraft with intact, partially failed, and fully failed repairs. Emphasis has been placed on investigating methods and tools used to conduct analysis and performance predictions of failed bonded repairs as well as those used to monitor and evaluate repair quality over the life of the part. Current efforts support compliance to the FAA's bonded repair size limit (BRSL) policy, with methods for predicting the residual strength for a failed repair in solid composite laminates having full-depth, half-depth, and double-sided scarfed configurations. In general, methods under development for residual strength predictions for failed bonded repairs correlated well with test results. Results reveal increased residual strength capability by keeping parent material intact during the removal process, i.e., partial scarf configurations had better strength than full-depth scarf configurations. There was no reduction in residual strength due to fatigue after 3 design service goals (DSGs) under SL conditions for all panels and scarf configurations tested. A single-sided repair patch in a double-sided scarf panel tested in this program cannot be credited for restoring the strength

Keywords: Solid Laminates, Scarf Repairs, Bonded Repair Size Limits, Structural Test, Analysis Methods

INTRODUCTION

Composite materials has been used in aerospace structures for several decades and more recently, composites have found its place in primary structures (such as fuselage and wing) of the civil aircraft. Over 50% of structural weight of A350 and B787 is made of composite materials, mainly Carbon Fiber Reinforced Polymers (CFRP) [1].

During its operational life, an aircraft will likely sustain damage due to bird strike, hail damage, lightning strike, tool drop and other mechanical collisions. The traditional repair method to repair such damage is mechanically fastened repairs, which is very good and suitable for metallic structure. However, these repairs are not always feasible for composite structure due to skin thicknesses, unbalancing of stress distribution due to differences in mechanical properties of the materials and also stress concentration around the riveted holes [2]. In addition, drilling holes in composite structures require special tools and skills to avoid introducing delaminations and other damage in the laminate. A viable alternate to repair composite structures is bonded repair, which utilize the similar material repair and does not require drilling holes. Bonded repairs are preferred over bolted repairs due to their superior load transfer and aerodynamically flush surface [3]. The damaged area is removed from the structure of the parent structure and scarfing is conducted around the removed area. This allows a load transfer between the laminate and the bonded repair patch via shear loads [1, 2].

Although bonded repairs are very effective, there remain several challenges that limits the application of bonded repairs. One such challenge pertains to the integrity of the bond between the repair patch and the damaged structure, which depends on numerous installation parameters. Errors during installation, including exposure of the repair patch to a humid environment, improper surface preparation, contamination of the bondline, insufficient control of the curing temperature, or loss of vacuum pressure, can lead to a reduction in bondline strength. Furthermore, weak bonds cannot be detected by existing non-destructive inspection (NDI) techniques. Challenges like these makes it harder to maintain consistent process controls causing most aircraft manufactures to limit the use of bonded repairs [3]. Consequently, the Federal Aviation Administration (FAA) issued a policy statement regarding bonded repair size limits (BRSL) to primary structure [4], which requires that "All critical structures must have a repair size limit no larger than a size that maintains limit load residual strength capability with the repair completely failed or failed within arresting design structures." The policy further states that "to expand the size limits of a given bonded repair patch, repair designs must have structural substantiation based on tests or analyses supported by tests. Additional datasets are required to qualify bonded material and process compatibilities, to demonstrate the proof of structure, and to establish reliable inspection procedures." In other words, bonded repairs must be demonstrated to hold ultimate loads (defined as 1.5 times the maximum load expected to be seen in service) with the repair intact, and must hold limit loads (defined as the maximum load expected to be seen in service) with the repair failed between arresting features, or fully failed if there is no arrestment.

The FAA and The Boeing Company have collaborated in a research program to gain better insight into the strength and performance of different bonded repair configurations in the intact, partially failed, and fully failed condition in support of compliance to the FAA's BRSL policy. The focus has been on both test and analysis of bonded repairs to representative composite wing panels using the Aircraft Beam Structural Test (ABST) fixture [5], an innovative structural test capability at the FAA William J. Hughes Technical Center. The program objectives are to:

(1) Characterize the fatigue and damage tolerance performance of a typical composite wing panel of transport category aircraft with varying repair designs in the intact configuration when subjected to a simulated service load (SL).
(2) Evaluate the load capability of a typical composite wing panel of transport category aircraft with partial and fully failed repairs.
(3) Assess methods and tools used for the performance analysis and for evaluating and monitoring repair integrity.

This paper summarizes recent efforts to characterize limit load residual strength for partial and fully failed scarf repair configurations. Details are provided in [6 – 8]. In general, full-depth, half-depth and double-sided scarfs were inserted in carbon-fiber-reinforced polymer (CFRP) panels having an 18-ply quasi-isotropic layup to simulate a fully failed repair. A subset of the double-sided scarf panels were reinforced with a single-sided repair patch to simulate a partially failed repair. The panels were attached as top-side components (e.g., skins) of a cantilevered, 24-inch-wide by 40-inch-long wing box structure in the ABST fixture. These panels were subjected to constant moment loads and tested either quasi-statically to failure or subjected to fatigue before loading them to failure. The fatigue loading conditions simulated the highest operational strain levels for transport category wing panels for 165,000 cycles (equal to three design service goals (DSGs) in a typical transport category aircraft).

In general, results reveal:

(1) There is an increase in the residual strength capability of a repair by keeping parent material intact during the removal process (i.e., a half-depth scarf is stronger than a full-depth scarf).
(2) There was no reduction in strength due to fatigue after 3 DSGs in all panels and scarf configurations tested.
(3) A single-sided repair patch in a double-sided scarf panel tested in this program cannot be credited for restoring the strength.
(4) Methods presented here for bonded repair residual strength predictions correlated well with test results.

EXPERIMENTAL PROCEDURES

This section describes the experimental procedures used in this program, including the test fixture, panels, applied loads, and the inspection and monitoring methods.

Test Fixture Description

Testing was conducted by the FAA using the ABST fixture located at the FAA William J. Hughes Technical Center. The ABST fixture, shown in Figure 1, was developed in collaboration with The Boeing Company at the start of this program and can apply major modes of loading to panels representing a typical wing or stabilizer components. A detailed, component-by-component description of the ABST fixture and supporting systems are provided in [5].

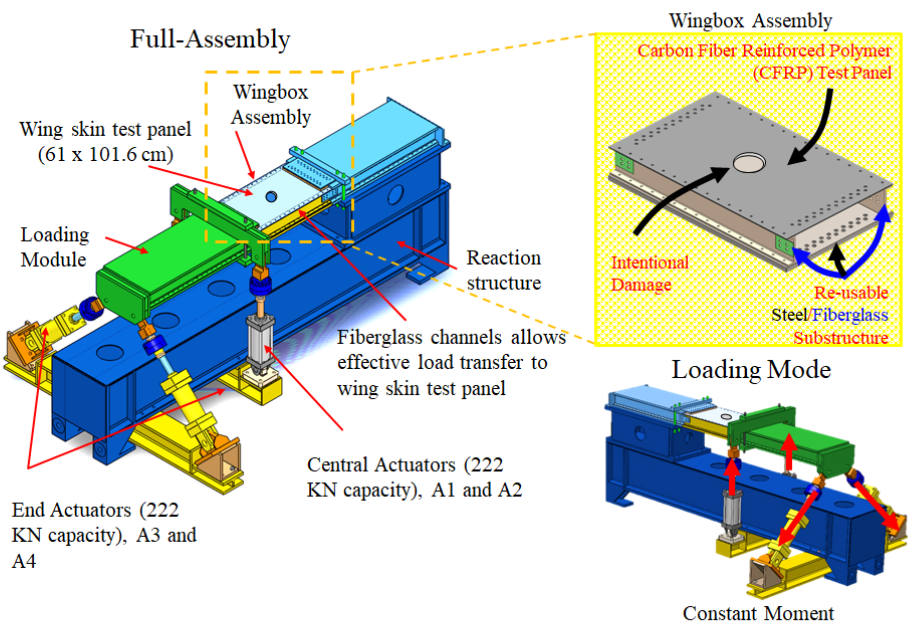

Figure 1. ABST Fixture assembly and examples of loading modes

Test Panel Description

The Boeing Company fabricated full-depth, half-depth, and double-sided scarfs in CFRP panels. The full test matrix is summarized in Table 1. The test articles were flat composite solid laminate panels (61.0-cm wide, 101.6-cm long, and 3.4-cm thick) representing typical skin panels of wing or empennage components. The panels were 18-ply quasi-isotropic lay-up, [±45°fabric/-45°/90°/45°/0°/-45°/90°/45°/0°]s. Panels were fabricated with a high modulus carbon/epoxy prepreg material, a typical material used by The Boeing Company for the composite primary structure of commercial applications. These panels had holes machined to match the fixture attachment points. The 61-cm long ends of the panel were reinforced with doublers (end tabs) for load introduction into the test article. These end tabs were made from the same material and lay-up as the test panel and included a taper region with ratios of around 30:1.

Table 1. Test Matrix

Panel No.	**Scarf Configuration**	**Load Type**	**Cross Sectional Schematic**
3	Half-Depth	Baseline Residual Strength	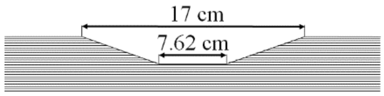
5	Half-Depth	Fatigue to 6 DSG (330,000 cycles) under 2,200 $\mu\varepsilon$ (SL conditions)	
		Post-Fatigue Residual Strength	
4	Full-Depth	Baseline Residual Strength	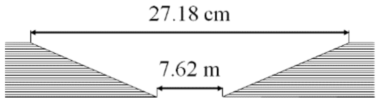
6	Full-Depth	Fatigue to 3 DSG (165,000 cycles) under 2,200 $\mu\varepsilon$ (SL conditions)	
		Post-Fatigue Residual Strength	
7	Double-Sided Scarf	Baseline Residual Strength	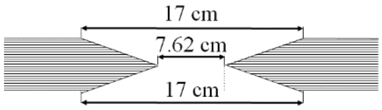
8	Double-Sided Scarf	Fatigue to 3 DSG (165,000 cycles) under 2,200 $\mu\varepsilon$ (SL conditions)	
		Post-Fatigue Residual Strength	
9, 10 & 11	Double-Sided Scarf w/ Single-Side Patch	Baseline Residual Strength: Compare with Half-Depth Scarf	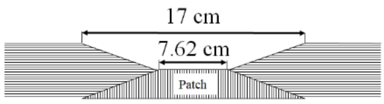

Images of the panels with the scarf configurations are illustrated in Figures 2 and 3. Altogether, nine 18-ply solid laminate panels were tested during this part of the program: Two with half-depth scarf (panels 3 and 5), two with full-depth scarf (panels 4 and 6), two with double-sided scarfs (panels 7 and 8), and three with double-sided scarfs (panels 9-11) with single-sided repair patches. The three panels with single-sided repair patch were fabricated by two separate organizations within The Boeing Company to account for potential variations in production processes. The scarf ratio for all panels was 30:1.

Applied Loads

The applied test loads used in this study represent the strains experienced by a composite wing panel of a typical transport-category aircraft, which usually includes compression, tension, and shear. Three loading types were considered:

(1) Strain survey loads applied quasi-statically to a percentage of the SL conditions (typically 75%–100% of the SL conditions) to ensure proper load introduction into the panel.
(2) Fatigue loads simulating normal operational or SL conditions during a flight cycle, the peak of which is estimated to be 37% of the ultimate load conditions (based on notched allowable coupons). If required, elevated fatigue loads were used to induce damage growth (40%–60% of the ultimate load conditions). Fatigue loading conditions did not consider scatter.
(3) Ultimate loads to measure residual strength applied quasi-statically.

A summary of these load configurations and the corresponding strain values is provided in Table 2. The tests covered in this report were for tensile loading conditions only. Further details of the applied loads used are provided in [6, 7].

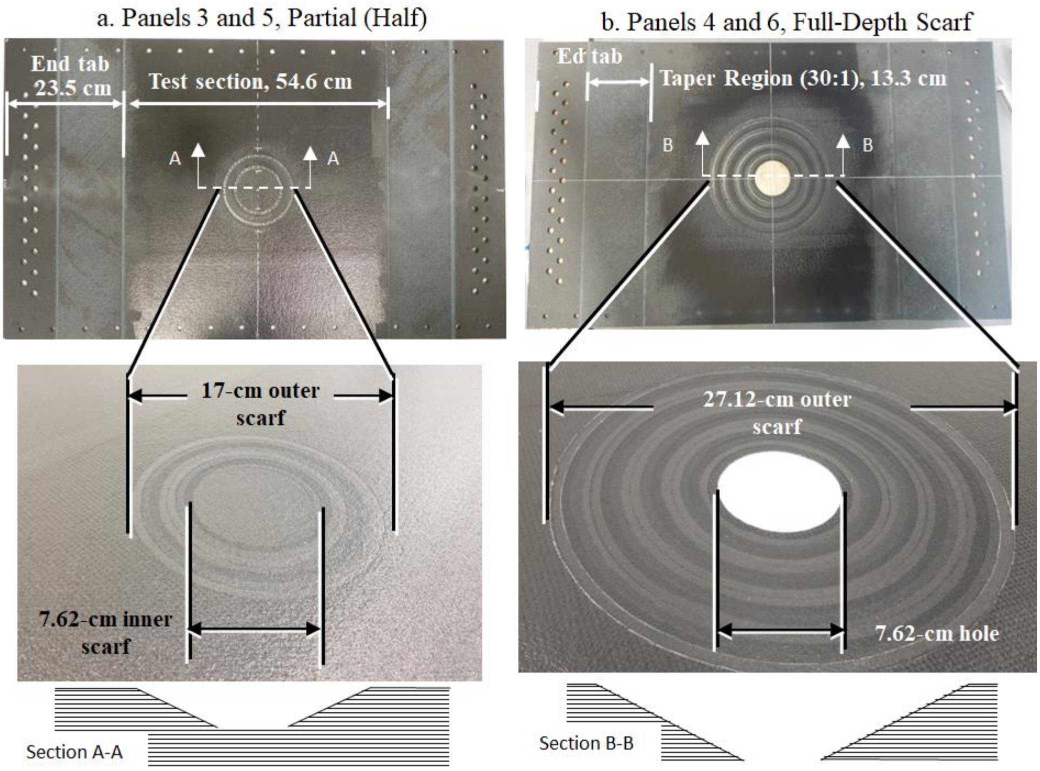

Figure 2. Panel configurations of panels 3-6.

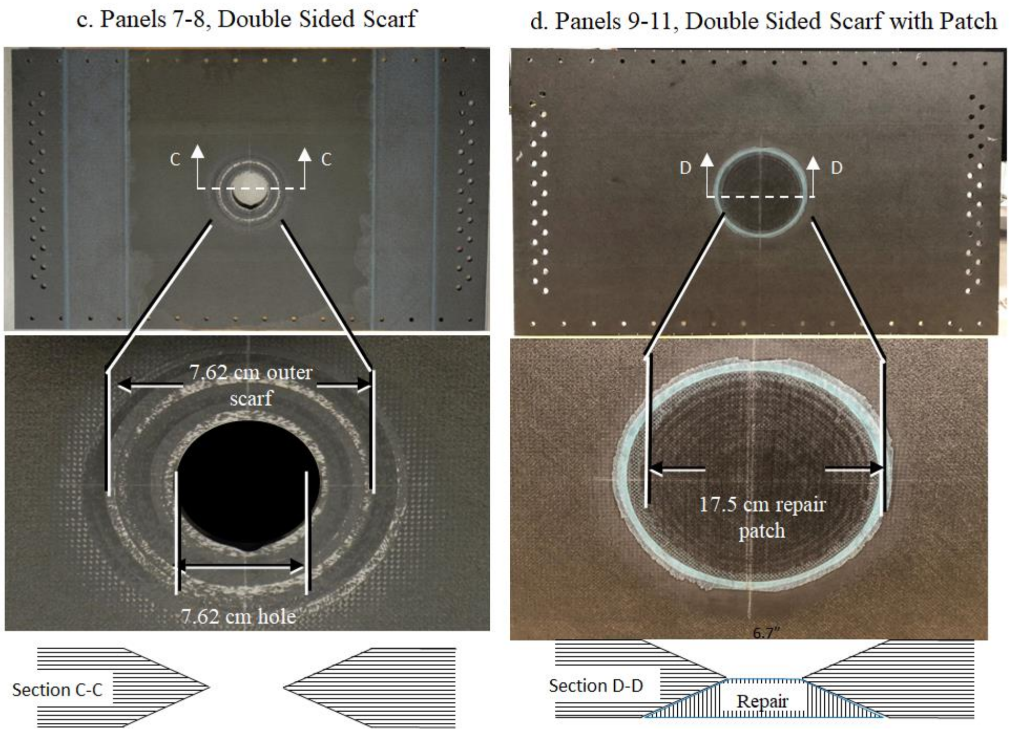

Figure 3. Panel configurations of panels 7-10.

Table 2. Strain levels used in program

Test Description	Load Type	Strains (με)
		Tension
Strain survey—75%–100% of the simulated SL strain conditions	Static	1,660 – 2,200
Fatigue—simulated SL conditions (37% of ultimate strains)	Cyclic (R = 0.1)	2,200
Fatigue—elevated loads to induce damage growth (40 - 60% of ultimate strain)	Cyclic (R = 0.1)	2,400 – 3,600
Residual strength (ultimate strains)— typical design ultimate loads of notched allowables	Static	6,000

Inspection and Monitoring Methods

During testing, several non-destructive inspection (NDI) methods were used to monitor and record the damage formation and growth, including thermography, phased-array ultrasound, pulse-echo ultrasound, and high-magnification cameras. In addition, panels were instrumented with strain gages and digital image correlation (DIC) systems to monitor strains throughout the tests. A commercial piezoelectric-based SHM system was also used to collect data and to assess its capabilities to monitor damage growth. Details are provided on [6, 7].

ANALYSIS PROCEDURES

Several analysis procedures were conducted by The Boeing Company in support of this program, as outlined in this section.

Finite Element Analysis

Finite element models (FEM) of the test fixture and test panels were created to simulate the loading of the panel prior to actual testing and provided predictions of: (1) actuator loads that the ABST fixture should apply to provide appropriate target strains; (2) stress and strain fields; (3) damage initiation and growth in the composite panel, and; (4) ultimate load and residual strength. Figure 4 shows an example of a full-depth scarf panel model under strain survey loading.

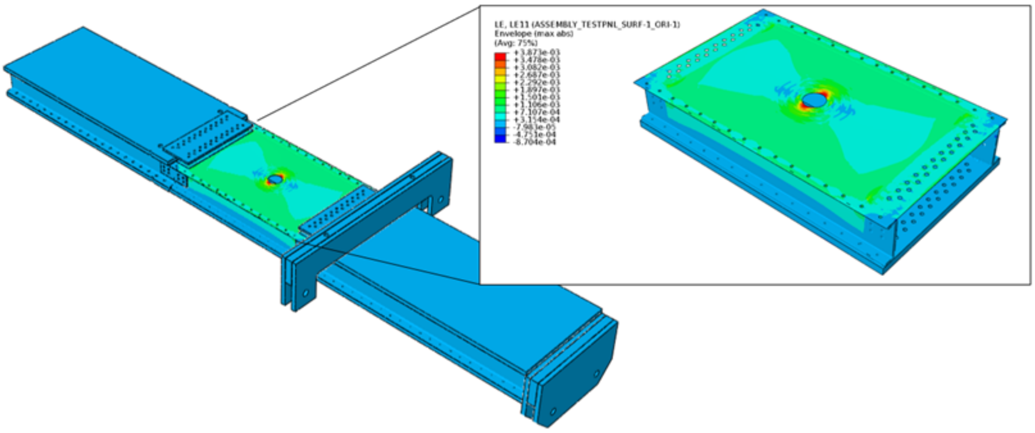

Figure 4. FEM used in test setup and pre-test prediction. Full-depth scarf panel with axial strain contour under 11,783 lbf-ft full-depth scarf [7]

An advanced progressive failure analysis (PFA) approach was used to predict the failure load levels for various scarfed panels in this test program. The current approach implements the Hashin in-plane failure criteria and the PFA input properties were derived from analysis and tests for the specific materials, processes and design practices. Figure 5 shows the matrix and fiber tensile failure index contours at failure load for a 30:1 scarf panel (only the damaged regions were shown).

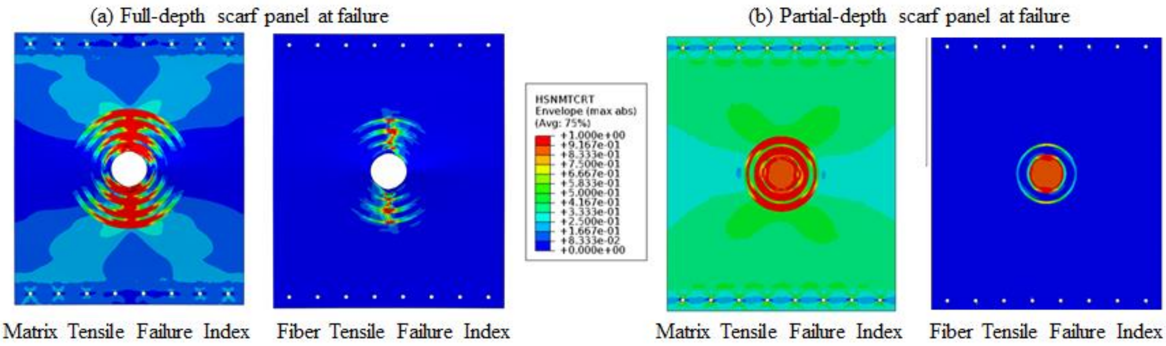

Figure 5. PFA approach to predict residual strength in Full-Depth and Half-Depth Scarf Panels

<u>BRSL semi-analytical method development and verification</u>

The development and verification of a rapid-executing K_t – based BRSL analysis method is being undertaken to predict the limit load residual strength for a failed scarf repair in solid composite laminates and honeycomb panels. It is based on the classic strain concentration factor K_{d0} approach modified by a geometry factor Ksr, as shown in Figure 6, under tensile loading. K_{sr} is obtained by three-dimensional finite element analysis, with extremely refined mesh around the scarf region to ensure the convergence of results. Depending on pristine and scarf repair design space, various non-dimensional parameters pertaining to scarf sizes, panel widths and scarf ratios are included in the K_{sr} function. The initial focus has been the limit load capacity (the maximum load to be expected in service) characterization for half- and full-depth scarf configurations for solid laminates under tension produced by constant moment. From the open-hole panel testing [6], the characteristic length parameter d_0 was found to be 1.27 mm for the specific laminate family tested and under room temperature ambient condition, based on equation (4) in Figure 6. Note that d_0 is material dependent parameter calibrated by test. In general, d_0 is a function of laminate layup, thickness, hole size, temperature and humidity. Caution needs to be exercised when applying this K_t-method: enough testing is needed to obtain d_0 to cover specific composite material systems, layups, damage sizes and environmental conditions. The following tests are recommended to obtain d_0:

(1) Unconfigured flat panels under tension, with three straight (non-scarfed) open holes of three different diameters that cover lower bound, intermediate, upper bound and practical damage sizes
(2) Repeat (1) for different laminate families with different layups (e.g., harder layups with more 0-degree plies for wing panels)
(3) Preferably (1) & (2) to be conducted under critical environmental conditions (e.g., elevated temperature wet (ETW))

Because of the significant change in skin stiffness implied in the fully disbonded full scarf scenario, loads are expected to re-distribute toward stiffening elements within the same panel, as well as to neighboring panels. A load redistribution factor can be calculated based on the EA (elastic modulus times cross-sectional area) for each component, by comparison between the intact and failed configuration magnitudes. The first step is to define the effective width that will remain constant for the total load calculation. Figure 7 shows the adjacent stiffeners and half the adjacent bay's skin. Assuming strain compatibility, the total load is apportioned according to extensional stiffness of each component (adjacent bay, stiffeners, scarf bay).

P_{TOTAL} (summation of P1 through P5) is assumed to remain constant. Component loads are calculated for both intact panel and failed scarf configurations. The equations below demonstrate how a load redistribution factor can be obtained. Subscripts I and F denote intact panel and failed scarf configuration respectively:

P_{I3} and P_{F3} are the segment axial load for the bay presenting a scarf cutout. P_{TOTAL} and all geometry and material inputs are known values. The values for the intact configuration can be determined by solving the set of corresponding equations. The values for the failed configuration can be determined in a similar fashion, after determining the unknown value φ, which is a function of scarf geometry. The load redistribution factor Y = LRF_3 for the failed bay is P_{F3} / P_{I3}.

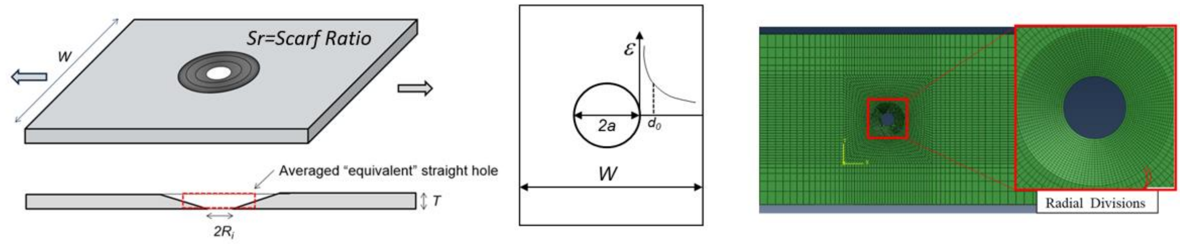

(1)Strain Concentration Factor (SCF)	$K_t = K_{d0}(K_{Sr})$
(2) Scarf Factor	$K_{Sr} = 1 + function(\frac{T}{Ri}, \frac{Ri}{W}, Sr)$
(3) Predicted failure strain	$\varepsilon_{scarf} = \varepsilon_{unt}/YK_t$ *Y is a configuration dependent load redistribution factor*
(4) Strain Concentration Factor for Straight Hole (d_0: Characteristic Length)	$K_{d0} = \frac{1}{2}C_w\left\{2+\left(\frac{a}{a+d_0}\right)^2 + 3\left(\frac{a}{a+d_0}\right)^4 - (K_T^\infty - 3)\left[5\left(\frac{a}{a+d_0}\right)^6 - 7\left(\frac{a}{a+d_0}\right)^8\right]\right\}$
(5) Edge Factor	$C_w = \left\{\frac{3(1-2a/W)}{2+(1-2a/W)^3} + \frac{1}{2}\left(\frac{2a}{W}M\right)^6 (K_T^\infty - 3)\left[1-\left(\frac{2a}{W}M\right)^2\right]\right\}^{-1}$
(6)Edge Factor Term M	$M^2 = \frac{\sqrt{1-8\left[\frac{3(1-2a/W)}{2+(1-2a/W)^3}-1\right]}-1}{2(2a/W)^2}$
(7) SCF for an infinitely large orthotropic plate	$K_T^\infty = 1 + \sqrt{2\left(\sqrt{\frac{E_x}{E_y}} - \nu_{xy}\right) + \frac{E_x}{G_{xy}}}$

Figure 6. Engineering approach based on K_t to predict residual strength [6]

Solving for a unit load for P_{TOTAL}

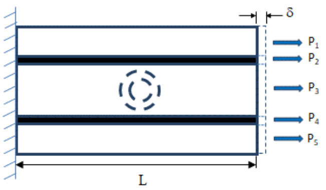

$$1 = P_{I1} + P_{I2} + P_{I3} + P_{I4} + P_{I5}$$
$$1 = \delta_I(A_1E_1 + A_2E_2 + A_3E_3 + A_4E_4 + A_5E_5)/L$$
$$\delta_I = L/(A_1E_1 + A_2E_2 + A_3E_3 + A_4E_4 + A_5E_5)$$

A_1 through A_5, E_1 through E_5, and L are known values.

$$1 = P_{F1} + P_{F2} + P_{F3} + P_{F4} + P_{F5}$$
$$1 = \delta_F(A_1E_1 + A_2E_2 + A_3E_3 + A_4E_4 + A_5E_5)/L$$
$$\delta_F = L/(A_1E_1 + A_2E_2 + A_4E_4 + A_5E_5 + E_3/[(L - 2R_0)/A_3 + 2\varphi/t_3])$$

A_1 through A_5, E_1 through E_5, t_3, R_0 and L are known values.
φ is numerically integrated from known values as well.

The load redistribution factor for the failed bay is the calculated ratio or the resulting P_{F3} and P_{I3}:

$$\boxed{LRF_3 = \left(\frac{\delta_F E_3}{[(L - 2R_0)/A_3 + 2\varphi/t_3]}\right)/(\delta_I A_3 E_3/L)}$$

Figure 7. A Schematic for calculating load redistribution factor Y

RESULTS AND DISCUSSION

Tests and analysis were performed to determine the fatigue and damage tolerance performance of CFRP panels with half-depth scarf (panels 3, 5), full-depth scarf (panels 4, 6), double-sided scarfs (panels 7, 8), and double-sided scarfs with single-sided repair patches (panels 9-11). Details can be found in [7, 8]. Representative results are presented in the subsequent sections.

Baseline Strain Surveys

Baseline strain surveys were conducted on all test panels to ensure proper load introduction. Strain survey loads were applied quasi-statically to a percentage of the SL conditions (typically 75%–100%) to achieve strain levels defined in Table 2. Representative results are shown in Figure 8 for Panel 5 having a half-depth scarf under an applied far-field target strain of 1800 $\mu\varepsilon$. Strain concentrations at the half-depth scarf were measured using DIC and strain gages. Figure 8a shows the location of strain gages and the DIC field of view. Figures 8b and 8c shows the axial strains measured via DIC and comparison of strain gage results and analysis predictions, respectively. In addition the axial strains measured via DIC along the section from 6 o'clock position to 12 o'clock position and strain gage S-11 are compared to the analysis predictions (Figures 8b and 8d). The test results had excellent agreement with the finite element analysis predictions.

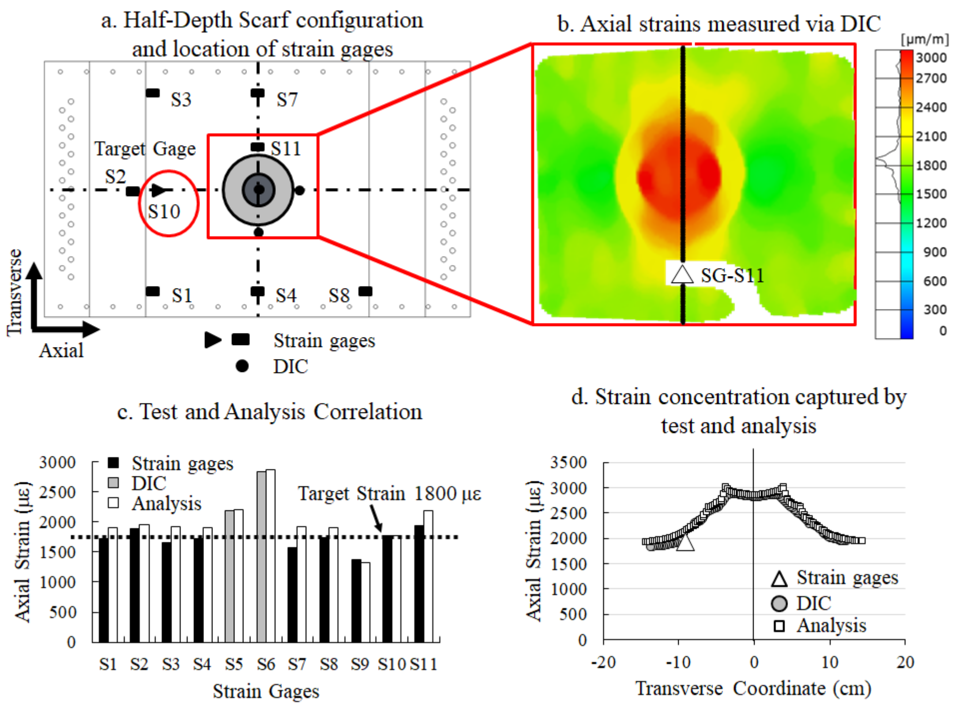

Figure 8. Baseline strain survey results for panel 5 – half-depth scarf.

Comparisons were made to the double-sided scarf panels with a repair patch (panels 9-11) as shown in Figure 9, that reveals a similar strain distribution. At the low applied load levels, the double-sided scarf with single-sided patch configuration works as the half-depth scarf configuration and shows similar strain distribution.

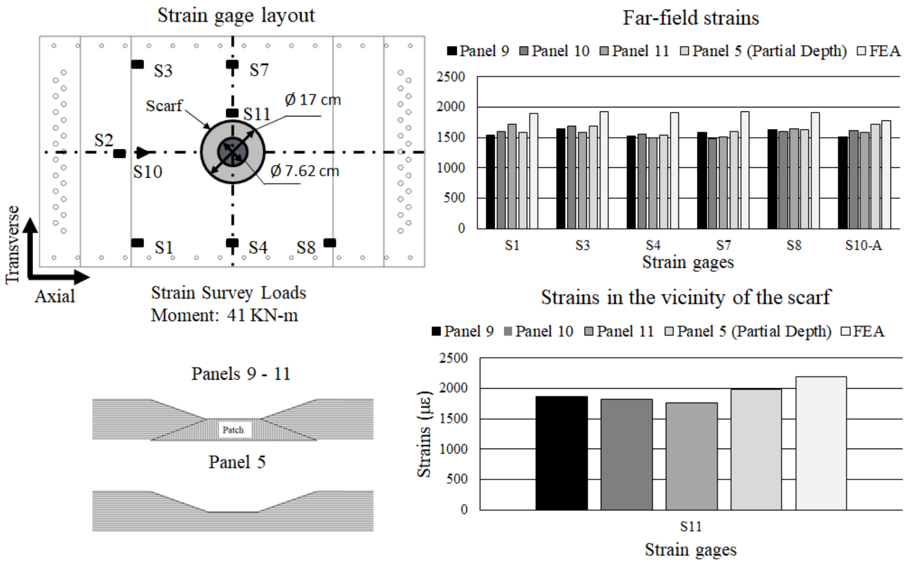

Figure 9. Comparison of strain survey results – double-sided scarf with a single-sided repair patch and half-depth scarf.

Effect of Fatigue

After the initial strain surveys, a subset panels indicated in Table 1 were subjected to at least three DSGs, i.e. 165,000 fatigue cycles at target maximum far-field strain of 2,200 με and R=0.1. In general, damage did not form under fatigue at SL conditions and had no effect on strain. Representative results are shown in Figure 10 for panel 8 having double-sided scarf. As shown, no strain redistribution was observed during the fatigue cycles as shown by DIC and strain gage results where the strains remained relatively similar throughout fatigue. During the tests, the panel was also inspected using a flash thermography system and the inspection results indicted a few small delaminations at 5 o' clock and 11 o' clock locations (Figure 10e). These delaminations were too small to have any effect on the durability of the scarf. In addition, the crack in the middle ply (0º ply) along the inner edges of the scarf did not grow due to fatigue, as shown in Figure 10. Overall, the double-sided scarf panel was able to sustain 3 DSGs without any new damage formation or growth.

Residual Strength

After the initial strain surveys and applied fatigue load (fatigue loads for panels 5, 6 and 8 only), all panels were subjected to a residual strength test, where the panels were loaded quasi-statically in a saw-tooth profile, incrementally increasing the applied load to failure. Typical results are shown in Figure 11 for the Panel 4 having a full-depth scarf. First visual indication of the damage was seen at 60% load increment in the form of cracking at the inner scarf edge at the 12 o'clock position. On increased load (70% load increment), damage progressed through the net section up to the middle 0° plies, which delaminated further at 80% load level but the damage was still contained within the scarf. At the 6 o' clock position, first delamination was observed at 70% load increment. Progressive damage growth occurred in this position through the entire net section of the scarf region during 80% load increment. Final failure occurred at 85% of the predicted strength through the net section of the panel.

Of particular interest, was the residual strength tests of the double-sided scarf with single-sided patch panels. The goal for panels 9-11 was to determine their ability to restore strength compared to the panels with half-depth scarfs (panels 3 and 5). These panels were loaded quasi-statically in a saw-tooth profile, increasing the load level up to the critical loads of the half-depth scarf, which was considered as 100%. Unexpectedly, all three panels failed at much lower load level. As shown in Figure 12, damage in Panel 9 at 35% load level in the form of edge delamination (first 0º ply) along the scarf inner-edge, at the 3 o'clock position. As the delamination was detected, the test was unloaded, and thermography inspection was conducted to document the delamination. The panel was then reloaded to higher load level and at 42% load level, the patch unexpectedly failed.

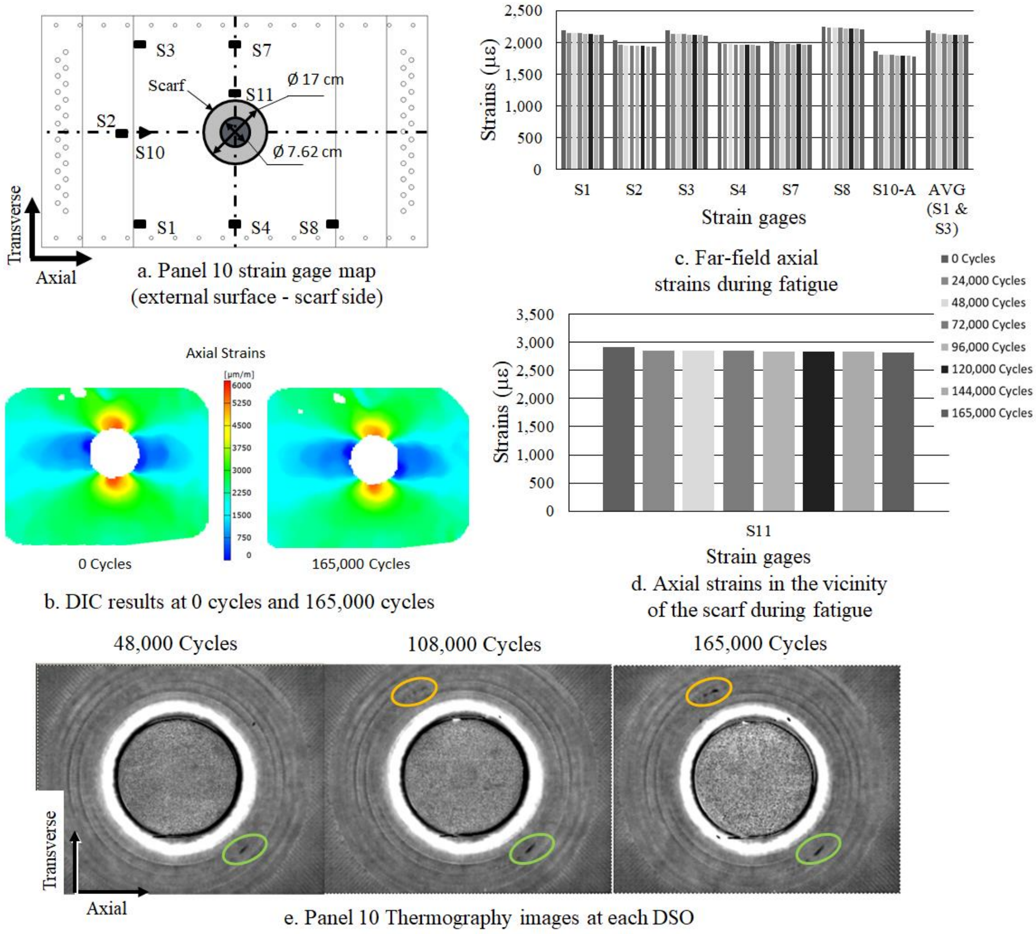

Figure 10. Effect of fatigue – Panel 8 doubler sided scarf.

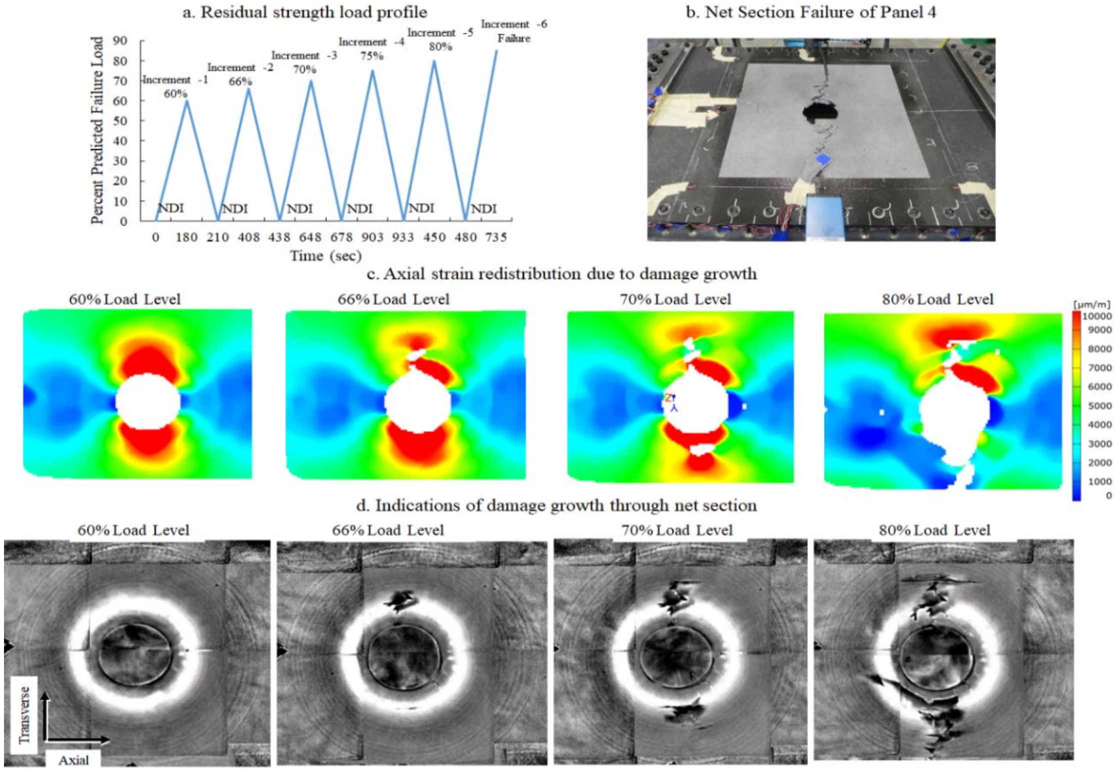

Figure 11. Panel 4 (full-depth scarf panel) results during residual strength test

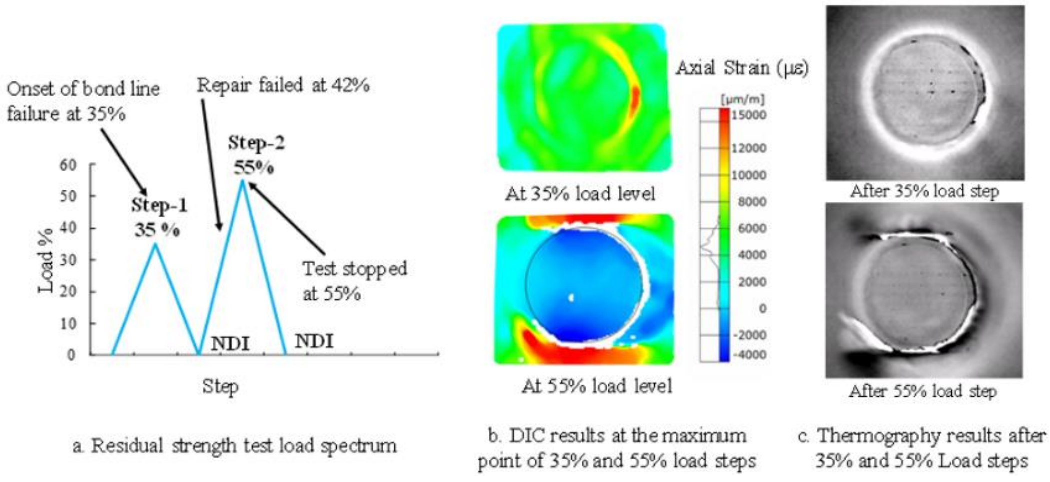

Figure 12. Panel 9, double-sided scarf with single-sided patch residual strength test

The test was subsequently stopped at 55% load level to save the panel for future inspections. Images of failed repair in panel 9 is shown in in Figure 13. The pictures of the interface between the patch and scarf shows the bondline failure and separation between the patch from the parent material and thus transferring the load to the net section, which would have soon led to the catastrophic failure of the panel if the test was not stopped.

It was decided to test two more panels (panels 10 and 11) fabricated at two separate labs at The Boeing Company to account for potential variations in production processes. Panels 10 and 11 were subjected to similar residual strength and subsequently failed suddenly at 59% and 58% of half-depth scarf.

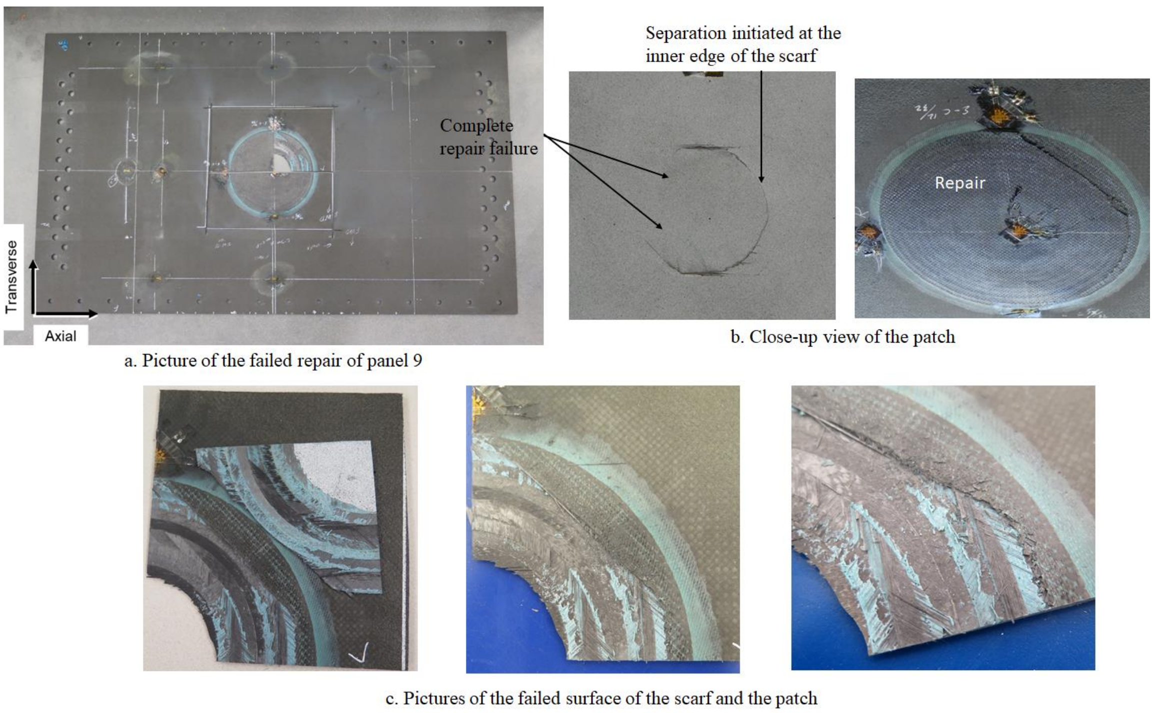

Figure 13. Post-failure pictures of panel 9

The bondline failure can be explained via Figure 14. As shown in the figure, a single-sided repair patch resulted in an eccentrically loaded moment and higher peel stresses causing the bondline failure. It should be mentioned that there was no substructure in these panels. The presence of stringers would have reduced the eccentricity and peel stresses on the bond by transferring more load on the stringer and reducing the prying moment.

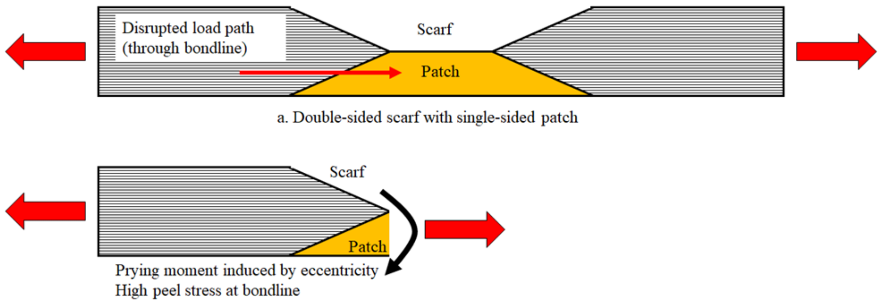

Figure 14. Schematics showing the prying moment induced by the eccentricity

A comparison of the residual strength for all panels is illustrated in Figure 15, showing the effect of notch geometry and fatigue. These strengths are normalized by the strength of an open-hole panel tested in [6]. For all panels, there was no reduction in residual strength due to fatigue after 3 DSGs. The increased in the residual strength capability of half-depth scarf panels 3 and 5 was revealed. This suggest that it's good practice to keep parent material intact during the scarf process. Benefits realized by double-sided scarfing include less material removal, a smaller repair footprint and consequently a slightly higher residual strength compared to a full-depth scarf configurations as shown in Figure 15.

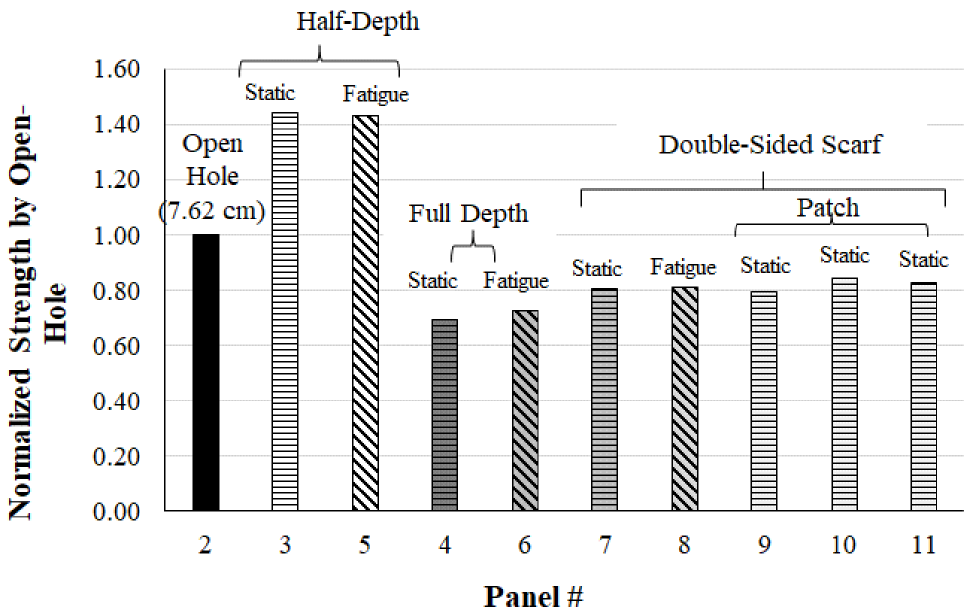

Figure 15. Panel 4 (full-depth scarf panel) results during residual strength test

The goal for the double-sided scarf with single-sided patch (panels 9-11) was to determine their ability in restoring the strength when compared to the panels with half-depth scarfs (panels 3 and 5). As shown earlier in Figure 9, at low load levels, the single-sided repair patch in a double-sided scarf was effective in restoring load transfer similar to that observed in the half-depth scarf panel. However, results in Figure 15 show that a single-sided repair patch in a double-sided scarf tested in this program cannot be credited for restoring the strength of the panel. Bondline failure of the repair patch occurred at the same load level as net section failure for the double-sided scarf configurations due to high peel stresses induced by bending eccentricity. It should be noted that these experiments were limited to 18-ply CFRP panels without any stiffening sub-structure, which does not represent an actual configured wing panel. For such structure, the stiffening elements (stringers, ribs, etc.) would in many cases react most of the bending moment, thus mitigating the effect of any eccentricity within the panel. While these results provide valuable insights to the residual strength behavior of CFRP panels with various scarf configurations, caution must be exercised in their direct application to real structure.

Test and Analysis Correlation

Using the K_t - based approach and PFA analyses, the effect of notched geometry on the failure strength of the solid laminates tested in this program was predicted as summarized in Figure 16. As shown, good agreement was obtained between the test and both analysis methods. The ultimate strains measured in Panel 3 containing a half-depth scarf was highest, as expected, followed by Panel 2 with the center hole and then Panel 4 containing the full-depth scarf. The benefit gained in the residual strength capability of the failed half-depth scarf is evident because it is much higher than the open-hole. Model predictions also show reduction of the stress concentration factor, K_t, as the scarf depth decreases.

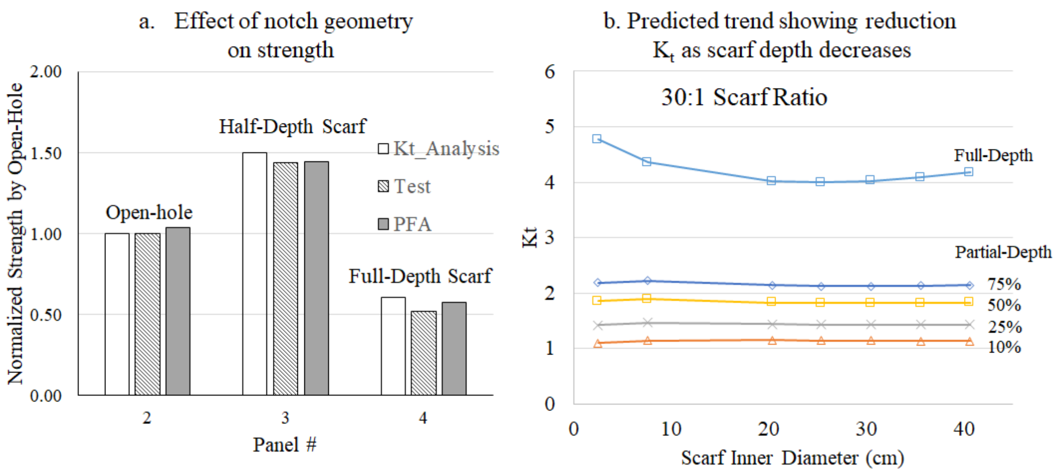

Figure 16. Kt-based approach and PFA used to predict residual strength and effect of scarf depth.

CONCLUDING REMARKS

In a collaborative effort, the FAA and The Boeing Company are assessing bonded repair technologies of composite panels representative of transport airplane wing structures through test and analysis using the FAA's ABST fixture. Emphasis has been placed on investigating methods and tools used to analyze and predict structural performance of bonded repairs and those used to monitor and evaluate repair quality and durability over the life of the part.

Results reported here support compliance to the BRSL policy with methods used to predict the residual strength for failed scarf repair configurations. Full-depth, half-depth and double-sided scarfs were inserted in carbon-fiber-reinforced polymer (CFRP) panels having an 18-ply quasi-isotropic layup. The panels were attached as top-side components (e.g., skins) of a cantilevered, 24-inch-wide by 40-inch-long wingbox structure. These panels were subjected to constant-moment loads applied either quasi-statically to failure or subjected to fatigue before being loaded to failure. The applied fatigue loading conditions simulated normal operational strain levels for transport-category wing panels for 165,000 cycles, which is approximately equal to three design service goals (DSGs).

In general, methods under development for BRSL residual strength predictions correlated well with test results. Results reveal benefits in the residual strength capability by keeping parent material intact during the removal process. There was no reduction in strength due to fatigue after 3 DSGs in all panels and scarf configurations tested. A single-sided repair patch in a double-sided scarf panel tested in this program cannot be credited for restoring the strength. Bondline failure of the repair patch occurred at the same load level as net section failure for the double-sided scarf configurations due to high peel stresses induced by bending eccentricity. It should be noted that these experiments were limited to 18-ply CFRP panels without any stiffening sub-structure, which does not represent an actual configured wing panel. For such structure, the stiffening elements (stringers, ribs, etc.) would in many cases react most of the bending moment, thus mitigating the effect of any eccentricity within the panel. While these results provide valuable insights to the residual strength behavior of CFRP panels with various scarf configurations, caution must be exercised in their direct application to real structure.

REFERENCES

[1] Schmutzler, H and Maier, A (2018); Automated Scarfing: A Prerequisite for Future Structural CFC Repairs, North Atlantic Treaty Organization Science and Technology Organization.
[2] Burka, P and Fischbach, F (2018); Structural Out-of-Autoclave Repair of Aircraft Fuselages via Adhesive Bonding, North Atlantic Treaty Organization Science and Technology Organization.
[3] Ashforth, C and Ilcewicz, L (2018); Certification of Bonded Aircraft Structures and Repairs, North Atlantic Treaty Organization Science and Technology Organization.
[4] Federal Aviation Administration. (2014); Bonded repair size limits. FAA Policy Statement No. PS-AIR-20-130-01, U.S. Department of Transportation.
[5] DOT/FAA/TC-TN19/7 (2019); Overview of ABST Fixture, https://rosap.ntl.bts.gov/view/dot/57880
[6] DOT/FAA/TC-21/17 (2020); Baseline Testing: Pristine and Open Hole, https://rosap.ntl.bts.gov/view/dot/61458
[7] DOT/FAA/TC-21/27 (2021); BRSL for Solid Laminates with Scarf Configurations: Full and Partial Depth, https://rosap.ntl.bts.gov/view/dot/60942
[8] DOT/FAA/TC-22/17, (2022); BRSL for Solid Laminates with Scarf Configurations: Double Sided Scarf, https://www.tc.faa.gov/its/worldpac/techrpt/tc21-17.pdf